

PACS numbers: 42.60.Da; 42.62.Eh; 07.07.Df; 42.81.Pa
DOI: 10.1070/QE2014v044n12ABEH015397

Super-large optical gyroscopes for applications in geodesy and seismology: state-of-the-art and development prospects

A.A. Velikoseltsev, D.P. Luk'yanov, V.I. Vinogradov, K.-U. Schreiber

Abstract. **A brief survey of the history of the invention and development of super-large laser gyroscopes (SLLGs) is presented. The basic results achieved using SLLGs in geodesy, seismology, fundamental physics and other fields are summarised. The concept of SLLG design, specific features of construction and implementation are considered, as well as the prospects of applying the present-day optical technologies to laser gyroscope engineering. The possibilities of using fibre-optical gyroscopes in seismologic studies are analysed and the results of preliminary experimental studies are presented.**

Keywords: *super-large laser gyroscopes, fibre-optical gyroscopes, geodesy, seismology, stabilisation, sensitivity improvement.*

1. Introduction

After the first successful demonstration of a laser gyroscope (LG) in 1963, its further development was determined mainly by the demands of inertial navigation, which in turn required the reduction of the influence of the lock-in zone on the gyroscope output, the instrumental mass and size. The possibility of using LG as a high-precision active interferometer for detecting super-small angular velocities was not considered for rather long time. In the late 1980s the research team from the University of Canterbury (Christchurch, New Zealand) launched a series of experiments to construct a 'large' LG aimed at solving a rather ambitious problem of testing the relativity theory [1].* The idea was to reach high sensitivity of the LG at the expense of enlarging its perimeter and eliminating intracavity elements thus improving the Q-factor of the resonator. In 1989 the LG with the cavity area 0.748 m^2 (the perimeter 3.47 m) was built, which allowed recording the angular velocity of the Earth rotation without using nonreciprocal elements [2]. Later this research team, with participation of the scientists from the State University of Oklahoma (USA), the Technical University of Munich, and the Federal Agency for Cartography and Geodesy of Germany, designed and built more perfect LGs with the cavity perimeter from 4 to 121.4 m [3–7].

* It is worth noting that the first LG, designed and fabricated by Macek and Davis 50 years ago, was at the same time the largest one. In 1963 its cavity had the shape of a rectangle with the perimeter 4 m and four gas discharge tubes, one in each arm nearly 1 m long. Here, apparently, the experience of creating the first linear gas lasers in 1960 had played its role.

A.A. Velikoseltsev, D.P. Lukyanov V.I. Ulyanov (Lenin) Saint Petersburg State Electrotechnical University LETI, ul. Prof. Popova 5, 197376 St. Petersburg, Russia; e-mail: avelikoseltsev@gmail.com, dplukyanov@mail.ru;
V.I. Vinogradov JSC Tambov Factory Elektropribor, Morshanskoye shosse 36, 392000 Tambov, Russia;
e-mail: valentin.vinogradov@gmail.com;
K.-U. Schreiber Forschungseinrichtung Satellitengeodaesie, Technische Universitaet Muenchen, Geodaetisches Observatorium Wettzell, Sackenrieder str. 25, 93444 Bad Koetzting, Deutschland;
e-mail: schreiber@fs.wettzell.de

Received 29 January 2014; revision received 15 July 2014
Kvantovaya Elektronika **44** (12) 1151–1156 (2014)
Translated by V.L. Derbov

2. Basic results achieved using super-large LGs

The permanent improvement of large LG (LLG) construction in combination with the enlargement of their perimeter using novel high-quality optical mirrors led to unprecedented sensitivity, allowing the registration of short-period variations of the angular velocity vector of the Earth [8, 9], which is illustrated in Fig. 1. In this Figure the data from the LLG G, obtained during 20 days, are presented together with the data of the model daily motion of the Pole for the same time period. It is seen that the data of the measurement agree well with those of modelling, and minor disagreements are caused either by real processes, such as the variation of weather conditions, deformation of the Earth surface, or laser artefacts.

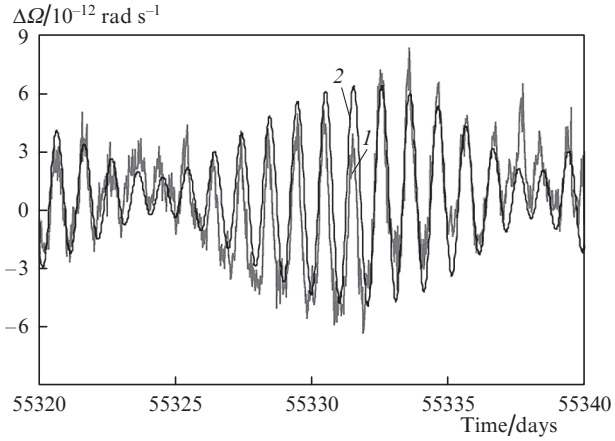

Figure 1. Output signal of the LLG G (*1*) and the data of the daily polar motion model (*2*). The data are presented in the angular velocity units after compensating for the steady component of the Earth angular velocity. The time is a modified Julian date (the days counted from the 16–17 November midnight, 1858).

Traditionally, the determination of the Earth orientation parameters (the length of day and the Pole coordinates) is implemented by means of very long baseline interferometry (VLBI). It is a complex system of coordinated radio telescopes, distributed over the planet surface. Large LGs can record the variations of these parameters by point measurements in real time. The output signals from the LLG G and the VLBI are presented in Fig. 2. Here curve (*2*) presents the results of the measurements of the Earth rotation parameters using the VLBI, namely, the variations of the Pole coordinates, recalculated into the units of angular velocity. Curve (*1*) shows the variations of the Earth angular velocity, measured with the LLG. The temporal interval in Fig. 2 equals ~60 days. The observed trend of the data from the LLG G and the VLBI coincides with the Chandler and annual motion of the Pole [10], the total period of which amounts to 428 days. It is worth noting that the VLBI generates data twice a week, while the LG measures the angular velocity every hour. The noise in the LLG output signal is caused by small oscillations of the perimeter, which cause a random variation of backscattering parameters.

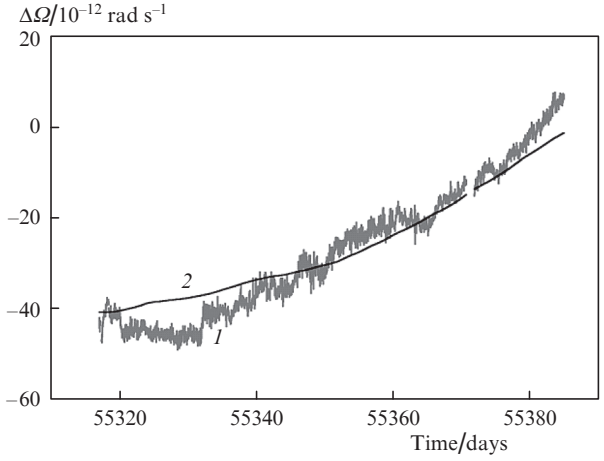

Figure 2. Output signals of the LLG G (*1*) and VLBI (*2*), illustrating the Pole motion with the Chandler period. The data are resented in the units of measurement of angular velocity after compensating for the steady component of the Earth angular velocity and its short-period variations. The time is a modified Julian date (the days counted from the 16–17 November midnight, 1858).

With LLGs the rotational components of seismic waves were also first detected [11–13], which earlier were considered to be negligibly small and playing no role in seismologic studies. The analysis of the data set on linear and rotational components of seismic signals has shown the possibility of obtaining new information about the Earth interior structure, which can be somewhat difficult using only traditional seismometers [14–16].

Most of the working LLGs are designed within one concept: the rectangular cavities are formed by four mirrors with low (smaller than 50×10^{-6}) losses. Intracavity elements are absent and all cavities are filled with the He–Ne gas mixture with equal content of neon isotopes. The optical pumping is implemented by means of a high-frequency discharge in the microwave range. The gas mixture pressure (~4–8 mbar) is increased to provide greater homogeneous broadening of the neon spectral line. The single-mode continuous-wave regime of laser operation is implemented by limiting the gain, such that all longitudinal modes except one are suppressed by choosing the active medium pump power (see Section 3 of the present paper).

With respect to construction, the LLGs can be divided into the monolithic ones (models C-II and, partially, G) and modular ones (models GEOsensor, G-0, UG1 and UG2). Monolithic devices are made of the material with a low thermal expansion coefficient (Zerodur), while modular ones are made of special vacuum tubes, connecting the corner chambers with mirror holders. The main parameters of existing large gyros are summarized in Table 1, taken from [17].

The limit sensitivity of the LG in the absence of technical fluctuations is determined by the quantum noise, and in the case of measuring the velocity of rotational motion can be presented as

$$\delta\Omega = \frac{cL}{4AQ}\sqrt{\frac{hf}{Pt}},$$

where c is the velocity of light; L is the cavity perimeter; A is the area bounded by this perimeter; Q is the cavity Q-factor; h is the Planck constant; f is the oscillation frequency; P is the power inside the cavity; and t is the time of averaging. The Q-factor of the LLG cavity is found by measuring the life time τ of photons in the cavity, as $Q = 2\pi f\tau$. The oscillation power P is found from the power P_{out}, measured at the output of the LG and the photon life time τ as $P = P_{\text{out}}L/(cT\tau)$, where T is the known transmission coefficient of the mirror. The calculated values of the LLG limit sensitivity are presented in Table 1 [17].

To date the fields of LLG application are geodesy, seismology and fundamental physics. The goals of the studies are the further increase in the sensitivity of LLGs and their long-time stability. The first will provide the possibility to measure the variation in length of day to values of the order of 10 μs or shorter, which will allow increased precision of determination of the Earth orientation parameters in combination with the VLBI [18]. The second will lead to reliable detection of low-frequency geophysical signals, caused by the Earth's tides,

Table 1. The main LLG parameters.

Model	Cavity loop area/m^2	Cavity loop perimeter/m	Q-factor	Beating frequency/Hz	Sensitivity/rad s^{-1}
C-II	1	4	5.3×10^{11}	79.4	146.2×10^{-12}
GEOsensor	2.56	6.4	3×10^{12}	102.6	108.1×10^{-12}
G-0	12.25	14	2.5×10^{12}	288.6	11.6×10^{-12}
G	16	16	3.5×10^{12}	348.6	12×10^{-12}
UG1	367.5	77	1.2×10^{12}	1512.8	17.1×10^{-12}
UG2	834.34	121.4	1.5×10^{12}	2180	7.8×10^{-12}

variations of the ocean and atmosphere kinetic moments. Active studies are carried out in this direction; the stabilisation of the cavity contour is implemented using frequency combs and pressure control in the isolating containment [17]. Additional contours of active perimeter stabilisation already at present make it possible to provide oscillation frequency fluctuations limited within ±1 kHz [19]. A gradual increase in the LLG resolution is illustrated in Fig. 3. By using the above stabilisation measures and the upgrade of the device itself, it appeared possible to increase the sensitivity of LLG G by an order of magnitude, and practically approach the theoretical limit level, determined by quantum noise.

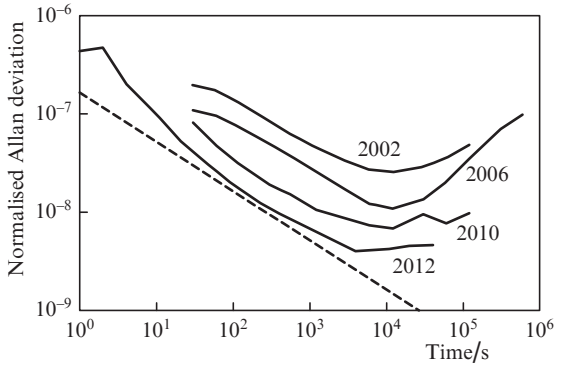

Figure 3. LLG G sensitivity characteristics, presented as Allan deviations, normalised to the mean velocity of the Earth rotation. The dashed line is the theoretical quantum limit for the considered instrument. Solid curves show the LLG sensitivity evolution in the course of its upgrade: non-stabilised LLG (2002), replacement of mirrors with better-quality ones (2006), improved perimeter stabilisation system (2010 and 2012).

3. Prospective optical technologies in the laser gyroscope engineering

One of the possible ways to increase the precision of the LLG operating in the continuous-wave regime is the reduction of losses at the cavity mirrors. In the process of exploitation of a UG-2 LLG with the perimeter of 121.4 m it was noticed that the cavity Q-factor was not as large as it could be expected in the LG of such size. This fact was interpreted as a consequence of high mirror losses, since the increase in the cavity arm lengths leads to the increase in the exposed area of the mirror surface [17]. The transverse size of the beam in the UG-2 LLG was beyond the mirror apertures, which led to the growth of diffraction losses. Therefore, it was concluded that a further increase in geometric dimensions of the cavity contour is not reasonable with the existing technology of dielectric mirror production.

The mirrors used in most LLGs are fabricated by means of tried-and-true technology of ion beam deposition of SiO_2/Ta_2O_5 layers onto a fused silica substrate and possess the losses $\sim 10^{-6}$. Such mirrors are currently used in interferometric detectors of gravitational waves and in optical atomic clocks. However, even the best samples of dielectric mirrors possess thermal noise that causes random vibrations of their surface, which makes a fundamental limitation of sensitivity in interferometric systems [20]. The existing methods of reducing the thermal noise essentially complicate the structure of the devices. In the case of large ring lasers the thermal noises of mirror coatings change the arm lengths of the cavity, which gives rise to random variations of the scale coefficient and the backscattering parameters.

Recently, a promising technology of optical mirror fabrication has been proposed [21]. It is based on using monocrystalline AlGaAs heterostructures as a material for forming the optical layers. On the base plate of gallium arsenide using the method of molecular beam epitaxy the quarter-wavelength layers of GaA (with a large refractive index) and AlGaAs (with a small refractive index) are grown. Then the structure is removed from the parent plate and is mounted on the permanent substrate using the connection, similar to the optical contact. The permanent substrate is made of polished silica glass. The obtained experimental samples of crystalline mirrors have the transmission losses 4×10^{-6}, the scattering and absorption losses being $\sim4\times10^{-6}$ and $\sim12\times10^{-6}$, respectively. The new mirrors demonstrated a tenfold reduction of the thermal noise level as compared to the dielectric ones. Further improvement of this technology will allow the fabrication of mirrors with low losses and the required curvature radius. At present the only drawback of this technology is that the reflection spectrum of crystalline mirrors lies in the IR region (1.03–1.14 μm). This circumstance complicates the visual control of the beam propagation in the cavity and its alignment. Nevertheless, the possibility of increasing the stability of optical frequency in the LG cavity due to the reduction of thermal noise effect seems to be a very promising direction of LLG development and requires experimental testing.

The increase in the LG perimeter leads to the decrease in the mode frequency separation which, in turn, requires reducing the excess of gain above the losses to provide the regime of single-mode oscillation. Thus, the increase in the perimeter in each of newly built super-large LGs was inevitably accompanied by lowering the power of laser radiation in the LG cavity. As a consequence, the questions arose about the potential limitations of the cavity perimeter in super-large ring lasers.

One of the possible limitations may be related to the character of the frequency spectrum excited in the LG cavity. We would like to remind that the number of modes arising in a cavity is, first of all, determined by the width of the active medium emission spectral line and the width of the interferometer resonance curve (Fig. 4) [22].

The number of oscillating modes with the frequencies ω_1, ω_2, …, ω_N is determined by the cavity perimeter L and the emission line width $\Delta\nu$

$$N = \frac{\Delta\nu}{c} L.$$

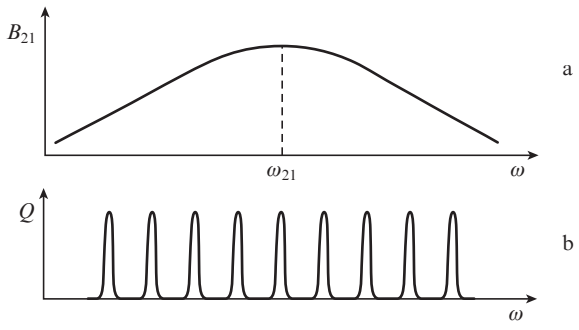

Figure 4. Dependence of the induced radiation coefficient B_{21} of Ne atom on the frequency ω (a) and the resonance curve of the interferometer (ring cavity) for the axial modes TEM_{00} (b).

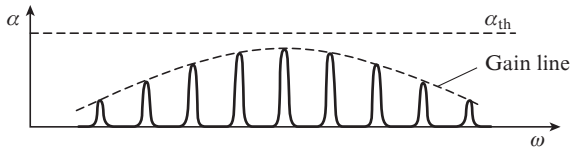

Figure 5. Dependence of the gain α on the frequency ω in the case, when the lasing threshold condition is not valid for any of the modes.

If the population inversion is so small that for none of the cavity modes the threshold condition is valid, then the oscillation is absent (Fig. 5).

With growing inversion the gain of the active medium increases, and the oscillation arises at the frequencies $\omega_1, \omega_2, \omega_3$ (Fig. 6). By choosing the gain one can obtain oscillation at a single frequency ω_2 and simultaneously suppress the oscillation at the frequencies ω_1 and ω_3.

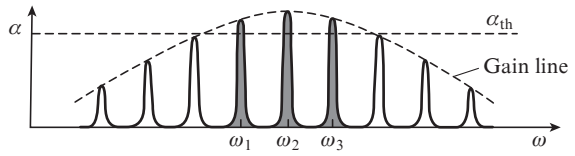

Figure 6. Same as in Fig. 5, but in the case when the lasing threshold condition is valid for the frequencies $\omega_1, \omega_2, \omega_3$.

However, this becomes more and more difficult as the perimeter L grows, when the overlap of amplitude-frequency characteristics of the adjacent modes occurs, and the traditional discrete line spectrum of the excited modes starts approaching a continuous one. Simultaneously with the spectrum broadening the power of single-mode radiation will decrease due to the necessity to select longitudinal modes with the frequencies, close to the oscillation frequency. This circumstance may be dominating among the limitations of extreme perimeter values in super-large LGs.

As an example, consider the estimated possibility of fabricating a super-large LG with the cavity, equivalent to the Michelson–Gale interferometer with the perimeter 1874 m (dimensions 603×334 m). In this case the mode separation c/L will amount to

$$\frac{3\times10^8\ \mathrm{m\ s^{-1}}}{1874\ \mathrm{m}} \approx 1.6\times10^5\ \mathrm{Hz} = 160\ \mathrm{kHz}$$

and will be smaller than the mode separation 18.75 MHz in the super-large LG of G type by more than two orders of magnitude.

At the same time, the results reported in Refs [23, 24] show that the maximal increase in the optical gyroscope sensitivity can be achieved by increasing the oscillation power in the cavity. The main problem is how to obtain the oscillation with a maximally high power in the spectral range with the width, equal to the collision-induced line width or smaller than it, without introducing additional optical elements into the cavity, which increase the cavity losses and complicate the LG construction.

In optics this problem is solved using an external cavity, coupled to the main one via a mutual mirror. With such a configuration of the optical scheme the oscillation is excited in a wide frequency range, and in the narrow region near the central frequency the oscillation is suppressed. In the case considered here an opposite effect is required, namely, the presence of single-mode oscillation in the vicinity of the central frequency of the lasing neon transition, and the absence of oscillation beyond this range. This can be achieved at the expense of the competition between the lasing transition $3S_2-2P_4$ ($\lambda_1 = 0.6328$ μm) and the optical transitions $3S_2-3P_4$ ($\lambda_2 = 3.39$ μm) or $2S_2-2P_4$ ($\lambda_3 = 1.1523$ μm), having a mutual upper ($3S_2$) or lower ($2P_4$) energy level with the lasing transition. In other words, if the auxiliary cavity with the appropriate parameters is tuned, e.g., to the wavelength of 3.39 μm, then at this wavelength no oscillation will occur in the main cavity within a certain frequency range due to high transmission losses (up to 92%) of the shared dispersion (coupled) cavity, but the oscillation at the main lasing transition with the lasing wavelength 0.63 μm will occur. In the rest of the frequency range (beyond the oscillation suppression zone) the competing radiation at the wavelengths 3.39 or 1.15 μm will be generated, which will suppress the oscillation at the lasing wavelength. The additional cavity has no effect on the operation of the main ring laser with $\lambda_1 = 0.63$ μm, since the radiation at this frequency is removed by means of a dispersion prism included in the auxiliary cavity and does not return back [25].

In the course of experimental studies the double-wave oscillation regime was implemented in a ring laser with the perimeter 200 cm simultaneously at two wavelengths (0.63 and 1.15 μm) using the mixture of helium and neon with equal content of isotopes. The stability of beat frequency was no worse than for single-wavelength operation at $\lambda_1 = 0.63$ μm.

Thus, it seem possible to increase the radiation power by a few orders of magnitude in one longitudinal mode of a super-large ring laser with significant reduction of the limit radiation line width and, correspondingly, with increasing the resolution power of these ring lasers. In this case no introduction of additional optical elements into the main cavity is needed. Clearly, the implementation of such operation regime with the high stability of indications being preserved will require additional experimental optimisation of parameters in super-large LGs with a coupled cavity.

Additional information about the double-frequency selection of longitudinal modes aimed at increasing the radiation power in the cavities of super-large LGs can be found in Ref. [25].

The transition to the pulsed regime [26] can be an efficient means of further sensitivity increase in super-large LGs. In this case two trains of short pulses are generated, propagating in the opposite directions in the closed loop. In the region of overlap an interference pattern is formed, which is used to estimate the beat frequency.

The potential advantages of using pulsed regimes is the essentially smaller degree of nonlinear coupling between the counterpropagating waves and the absence of competition between the counterpropagating modes in the active medium with homogeneous broadening. The presence of the Sagnac effect and the reduction of the lock-in zone in pulsed LGs were demonstrated in a number of studies [27–29]. These studies confirm the possibility of implementing an optical gyroscope using dye mode-locked lasers, as well as solid-state and fibre lasers. The studies carried out demonstrate the possibility to achieve the resolution of $\sim5\times10^{-13}$ rad s^{-1} [30]. In the case of using pulsed lasers in an optical loop with a large period it seems possible to obtain both the increased sensitiv-

ity of the LG and the reduced influence of backscattering on the output signal.

4. Fibre-optical gyroscopes as high-precision angular velocity sensors

Increasing the sensitivity of angular velocity optical sensors is possible not only by increasing the cavity size of the active ring interferometer. A widely used and prospective sensor is the fibre-optical gyroscope (FOG). The best models of commercial FOGs possess the drift level of $\sim 1.5\times10^{-9}$ rad s^{-1} [31, 32]. The advantages of the FOG include the possibility to obtain high precision in combination with small size, high technological effectiveness of production and relatively low cost. The increase in the sensitivity in a FOG, which is a passive optical interferometer, is achieved by increasing the length of light-guiding fibre and/or the diameter of the fibre coil. While in the navigation the increased device dimension is undesirable, in geodesy and seismology it does not play a crucial role. Therefore, it is possible to design FOGs with a sufficiently long fibre (a few kilometres) and with the coil diameter, exceeding the usual size (more than ten centimetres).

The experiment on assessing the possibility to increase the FOG scale factor by increasing the coil diameter was carried out in the Wettzell Geodesic Observatory (Germany). A single-mode fibre with the length of 2.2 km was wound around a glass-ceramic disc 4 m in diameter, which was a part of the LLG G. The obtained results allow the estimate of the resolution of such a FOG as 0.5×10^{-6} rad s^{-1} [18]. The output signal of the FOG is shown in Fig. 7.

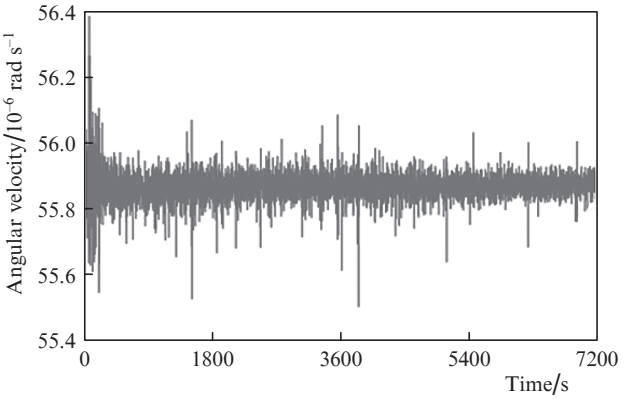

Figure 7. Output signal from the FOG with a large coil diameter. The mean value of the signal corresponds to the vertical projection of the Earth rotation velocity at the place of the instrument location.

It should be taken into account that the winding of the optical fibre was performed by hand, without using the quadrupole method, and the used light source was a small-power one. Hence, in spite of the formal enlargement of the big FOG scale coefficient by 143 times as compared to the LLG G, its sensitivity appeared to be by two orders of magnitude smaller than in the LLG due to high level of noise. The replacement of the light source with a superfluorescence one and the use of an improved digital control system are expected to increase the precision of this FOG. In the future a super-large FOG can be successfully used in seismologic studies, and the combination of its measurements with the LLG data will help in more precise characterisation of error in both instruments.

Alongside with the obvious increase in the measurement precision, the enlargement of the optical coil dimensions has drawbacks. In spite of the absence of general limitations imposed on the dimensions of measuring instruments in seismology, a number of research situations still require compact instrumentation. In particular, the compactness is necessary for operative and easy installation of FOGs in the regions of increased seismic activity. The use of LLGs is difficult in these cases, and they can be involved only as reference stations. It seems to be a compromise solution to use high-precision FOGs with relatively small dimensions [33]. At present the experiments on creating specialised FOGs for seismologic measurements are intensively carried out. A few FOGs are designed having the fibre coil diameter from 40 to 68 cm and the fibre length from 11 to 15 km. The sensitivity range is estimated by the authors as 2.3×10^{-6} – 5×10^{-9} rad s^{-1} [34, 35]. Due to significant coil dimensions the temperature effects exert essential influence on the output signal of large FOGs, and, therefore, in their construction the isolating Teflon layers and the quadrupole winding of the optical fibre are used. Such instruments can be successfully applied for recording rotational components of seismic waves in immediate proximity of the earthquake centre (near-field seismology).

In the future the progress in optical fibre production technology can bring the FOG to a new level. In particular, the use of a photonic crystal fibre promises numerous advantages in the implementation of optical angular velocity sensors. One of such fibres is the fibre with a photonic band gap in the definite wavelength range, in which the light can propagate along the core having the refractive index smaller than that of the cladding. Thus, the propagation of light in a hollow core (air) fibre becomes possible, which allows both the increase in the input radiation power and the significant reduction of nonlinear effects in such fibre [36]. This is favourable for better characteristics of a FOG using this type of optical waveguide. Experimental studies show that with the hollow core photonic crystal fibre in the FOG coil one can obtain the reduction of the Kerr effect by 170 times, of the Shupe effect by 6.5 times, and of the Faraday effect by 20 times [37]. For a gyroscope in 'minimal' configuration with the optical fibre length 235 m the sensitivity of $\sim 3.8\times10^{-6}$ rad s^{-1} was achieved, practically limited only by the excess noise of the radiation source. However, to date the hollow core photonic crystal fibres have high losses ($\sim$12–20 dB km^{-1}) and cost (\$500–\$1000 per 1 m). One can expect that with the progress of technologies the losses will be reduced; the fibre with the losses of $\sim$1.2 dB km^{-1} already exists, and further reduction of losses to 0.1 dB km^{-1} is expected [38]. The problem can be solved by improving the technological process, since the losses in the hollow core photonic crystal fibre are caused by the scattering of radiation due to the roughness of the waveguide channel surface.

The results of the studies, presented in Ref. [37], give rise to definite optimism about the prospects of developing the systems for detecting angular seismic vibrations, since the open loop FOG output signal provides the compatibility with the standard seismologic data acquisition systems. In the case of using a FOG with the closed loop scheme of output data processing (digital signal) the separate data acquisition systems are to be designed and constructed, which makes the use of optical sensors less attractive for the seismologic community. Thus, it seems promising to create FOGs of conventionally large diameter (tens of centimetres) with the coil of photonic crystal fibre.

5. Conclusions

The paper presents the state-of-the-art in the field of creating super-large LGs, aimed at high-precision measurements in geodesy, seismology and fundamental physics. Although at present such instruments demonstrate unprecedented resolution that allows detecting the oscillations of the Earth rotation vector in real time, the solution of the formulated problems requires further improvement of the LLG operating parameters. The major directions of research aimed at the LG sensitivity and stability improvement are presented. Also considered are the possibilities of using FOGs in high-precision measurements in geodesy and seismology, as well as the methods of increasing their precision characteristics.

Acknowledgements. In the present paper Sections 1 and 2 are carried out under the support from the Russian Scientific Foundation (Project No. 14-19-00693) and Sections 3, 4 and 5 under the support from the Ministry of Education and Science of the Russian Federation (Project No. 8.752.2014/K).

References

1. Stedman G.E. *Rep. Prog. Phys.*, **60** (6), 615 (1997).
2. Stedman G.E., Bilger H.R., Ziyuan L., Poulton M.P., Rowe C.H., Vetharaniam I., Wells P.V. *Austr. J. Phys.*, **46**, 87 (1993).
3. Schreiber K.U., Rowe C.H., Wright D.N., Cooper S.J., Stedman G.E. *Appl. Opt.*, **37** (36), 8371 (1998).
4. Rowe C.H., Schreiber U., Steven S.J., King B.T., Poulton M., Stedman G.E. *Appl. Opt.*, **38** (12), 2516 (1999).
5. Schreiber U., Velikoseltsev A., Klugel T., Stedman G.E., Schluter W. *Proc. Symp. Gyro Technology* (Stuttgart, 2001) pp 8.0–8.7.
6. Dunn R.W., Schreiber U., Steven S.J., King B.T., Poulton M., Stedman G.E. *Appl. Opt.*, **41** (9), 1685 (2002).
7. Hurst R.B., Stedman G.E., Schreiber K.U., Thirkettle R.J., Graham R.D., Rabeendran N., Wells J.-P.R. *J. Appl. Phys.*, **105** (11), 113115 (2009).
8. Schreiber K.U., Klugel T., Stedman G.E. *J. Geophys. Res.*, **108** (B2), 19 (2003).
9. Schreiber K.U., Velikoseltsev A., Rothacher M., Klugel T., Stedman G.E., Wiltshire D.L. *J. Geophys. Res.*, **109** (B6), B06405 (2004).
10. Schreiber K.U., Klugel T., Wells J.-P.R., Hurst R.B., Gebauer A. *Phys. Rev. Lett.*, **107** (17), 173904 (2011).
11. Stedman G.E., Li Z., Bilger H.R. *Appl. Opt.*, **34** (24), 5375 (1995).
12. McLeod D.P., Stedman G.E., Webb T.H., Schreiber U. *Bull. Seismol. Soc. Am.*, **88** (6), 1495 (1998).
13. Pancha A., Webb T.H., Stedman G.E., McLeod D.P., Schreiber K.U. *Geophys. Res. Lett.*, **27** (21), 3353 (2000).
14. Suryanto W., Igel H., Wassermann J., Cochard A., Schuberth B., Vollmer D., Scherbaum F., Schreiber U., Velikoseltsev A. *Bull. Seismol. Soc. Am.*, **96** (6), 2059 (2006).
15. Bernauer M., Fichtner A., Igel H. *Geophysics*, **74** (6), WCD41 (2009).
16. Hadziioannou C., Gaebler P., Schreiber U., Wassermann J., Igel H. *J. Seismol.*, **16** (4), 787 (2012).
17. Schreiber K.U., Wells J.-P.R. *Rev. Sci. Instrum.*, **84** (4), 041101 (2013).
18. Cerveira M., Schuh H., Klugel T., Velikoseltsev A., Schreiber U. *Proc. Fifth IVS General Meeting 'Measuring the Future'* (St. Petersburg, 2008).
19. Schreiber K.U., Gebauer A., Wells J.-P.R. *Opt. Lett.*, **38**, 3574 (2013).
20. Evans M., Ballmer S., Fejer M., Fritschel P., Harry G., Ogin G. *Phys. Rev. D*, **78**, 102003 (2008).
21. Cole G.D., Zhang Wei, Martin M.J., Ye Jun, Aspelmeyer M. *Nat. Photonics*, **7** (8), 644 (2013).
22. Batrakov A.S. *Kvantovye pribory* (Quantum Instruments) (Leningrad: Energiya, 1972).
23. Mazan'ko I.P., Molchanov M.I., Yaroshenko N.G. *Radiotekh. Elektron.*, **19** (8), 1698 (1974).
24. Vinogradov V.I. *Aviakosmicheskoye priborostroyeniye* (9), 8 (2005).
25. Vinogradov V.I. *Opt. Spektrosk.*, **111**, 1 (2011) [*Opt. Spectrosc.*, **111**, 139 (2011)].
26. Galkin S.L., Kruzhalov S.V., Nikolayev V.M., Pakhomov L.N., Petrun'kin V.Yu. *Pis'ma Zh. Tekh. Fiz.*, **2**, 150 (1976).
27. Dennis M.L., Diels J.-C.M., Lai M. *Opt. Lett.*, **16** (7), 529 (1991).
28. Lai M., Diels J.-C., Dennis M.L. *Opt. Lett.*, **17** (21), 1535 (1992).
29. Dennis M.L., Diels J.-C.M. *Appl. Opt.*, **33** (9), 1659 (1994).
30. Braga A., Diels J.-C., Jain R., Wang R.K.L. *Opt. Lett.*, **35** (15), 2648 (2010).
31. Sanders G.A., Szafraniec B., Strandjord L., Bergh R., Kaliszek A., Dankwort R., Lange C., Kimmel D. *OSA Technical Digest Series* (Williamsburg, OSA, 1997) Vol. 16, paper OWB1.
32. Honthaas J., Buret T., Paturel Y., Gaiffe T. *OSA Technical Digest Series* (Cancun, Mexico: OSA, 2006).
33. Velikoseltsev A., Schreiber K.U., Yankovsky A., Wells J.-P.R., Boronachin A., Tkachenko A. *J. Seismol.*, **16** (4), 623 (2012).
34. Jaroszewicz L.R., Krajewski Z., Solarz L., Teisseyer R. *Meas. Sci. Technol.*, **17** (5), 1186 (2006).
35. Jaroszewicz L.R., Krajewski Z., Kowalski H., Mazur G., Zinowko P., Kowalski J. *Acta Geophys.*, **59** (3), 578 (2011).
36. Cregan R.F., Mangan B.J., Knight J.C., Birks T.A., Russell P.S.J., Roberts P.J., Allan D.C. *Science*, **285**, 1537 (1999).
37. Digonnet M., Blin S., Kim H.K., Dangui V., Kino G. *Meas. Sci. Technol.*, **18** (10), 3089 (2007).
38. Roberts P.J., Couny F., Sabert H., Mangan B.J., Williams D.P., Farr L., Mason M.W., Tomlinson A., Birks T.A., Knight J.C., Russell P.S. *Opt. Express*, **13** (1), 236 (2005).